EFFECT OF HEAT SOURCE/SINK ON THE PERISTALTIC FLOW OF JEFFREY FLUID WITH SUSPENDED NANOPARTICLES IN AN ASYMMETRIC CHANNEL HAVING FLEXIBLE WALLS

V. P. RATHOD[1], D. SANJEEV KUMAR*[1, 2]

**[1]Department of Studies and Research in Mathematics,
Gulbarga University, Kalaburagi – 585 106, Karnataka, India.**

**[2]Department of Science,
Government Polytechnic, Aurad (B), Bidar, Karnataka, India.**

ABSTRACT

The effect of heat generation/absorption on the peristaltic flow of a Jeffrey fluid with suspended nanoparticles through an asymmetric channel, having flexible walls is considered. General boundary conditions on velocity, temperature and concentration of nanoparticles are considered. The contribution of nanoparticles to heat and mass transports are modeled by thermophoresis and Brownian diffusion effects. The governing equations of motion reduce to a system of partial differential equations under long wave length approximation and low Reynolds number limit. Closed form solutions of the resultant partial differential equations are presented for velocity, temperature and nanoparticle concentration distributions. Effects of various physical parameters like, Jeffrey fluid parameters, slip parameter, Biot numbers, thermophoresis parameter, Brownian motion parameters and heat source/sink parameter on velocity, temperature, nanoparticle concentration and pressure rise over a wavelength are discussed. The results of the paper may lead to possible technological applications in the field of biomedicine.

Keywords: peristaltic motion, asymmetric channel, micropolar fluid, nanoparticles.

1. INTRODUCTION

Peristalsis is a process that involves flow of a fluid in a tubular duct by the waves generated along the walls. Usually one encounters such motion in digestive tract such as the human gastrointestinal tract where smooth muscle tissue contracts and relaxes in sequence to produce a peristaltic wave, which propels the bolus (a ball of food) while in the esophagus and upper gastrointestinal tract, along the tract. The peristaltic movements not only avoid retrograde motion of the bolus but always keep pushing it in the forward direction, that is, the important aspect of peristalsis is that it can propel the bolus against gravity effectively. Peristaltic movements are effectively used by animals like earthworms and larvae of certain insects for their locomotion. Motivated by such biomechanisms, there are machineries that imitate peristalsis to cater for specific day-to-day requirements. Other important applications for peristalsis involves, movement of chyme in intestine, movement of eggs in the fallopian tube, transport of the spermatozoa in cervical canal, transport of bile in the bile duct, circulation of blood in small blood vessels and transport of urine from kidney to urinary bladder and so on.

Over past few decades, peristalsis has attracted much attention of a large class of researchers due to its important engineering and biomedical applications. Following the pioneering works of Latham [1], there have been several reports in literature on the theoretical and experimental studies concerning peristalsis mechanism. Peristaltic flow of Newtonian / non-Newtonian fluids in a symmetric channels / axisymmetric tubes has been extensively studied by several authors, Zien and Ostrach [2], Lee and Fung [3], Chaturani and Rathod [4], Srivastava *et al.*, [5], Takabatake *et al.*, [6], El Shehawey and Mekheimer [7], Ramachandra and Usha [8], Mekheimer [9], Misra and Pandey [10], Vajravelu *et al.*, [11], Mekheimer and Abd elmaboud [12], Rathod and Tanveer [13] and references therein. De Vries *et al.*, [14] have reported that the myometrial contractions may occur not only in symmetric channel but also in an asymmetric channel. With this view point there are quite a lot of studies in the literature related to the peristaltic flow of Newtonian/non-Newtonian fluids in an asymmetric channel, Ramachandra Rao and Mishra [15], Elshehawey, *et al.*,

Corresponding Author: D. Sanjeev Kumar[1, 2]
[2]Department of Science, Government Polytechnic, Aurad (B), Bidar district, Karnataka, India.

[16], Subba Reddy *et al.*, [17], Ali and Hayat [18], Ebaid [19], Sobh [20], Shit *et al.*, [21], Mekheimer *et al.*, [22], Srinivas and Muthuraj [23] , Srinivas *et al.*, [24], Das [25], Abd Elmaboud *et al.*, [26] and references therein. Recently, Yeng-Yung Tsui *et al.*, [27] studied the pumping flow in a channel with a peristaltic wall by comparing the numerical results with the theoretical predictions obtained from the lubrication model to determine the suitability of the proposed theory.

Current trends in nanotechnology research have lead to wide variety of potential applications in biomedical, optical and electronic engineering, material science, heat transfer engineering and so on. Nanofluid is a homogeneous mixture of particles of nanoscale and carrier fluids like water, ethylene glycol, oil and etc, which are commonly known as base fluids. As reported by Choi [28] it is an innovative technique to improve heat transfer by using nanoscale particles in the base fluid. Subsequently, Choi *et al.*, [29] showed that the addition of a small amount (less than 1% by volume) of nanoparticles to conventional heat transfer fluids increased the thermal conductivity of the fluid up to approximately two times. This innovation has created immense interest in the study of peristaltic flow involving nanofluids in symmetric/asymmetric channels; Akbar and Nadeem [30, 31], Akbar *et al.*, [32, 33], Mustafa *et al.*, [34], Beg and Tripathi [35].

There has been enumerable contribution by Rathod and his research group to the study of peristalsis through channels/annuli involving non-Newtonian fluids. Rathod and Channakote [36] have studied the effect of thickness of the porous material on the peristaltic pumping of a Jeffry fluid when the tube wall is provided with non- erodible porous lining. Peristaltic transport of couple stress fluid in uniform and non-uniform annulus through porous medium was considered by Rathod and Sridhar [37]. Rathod and Laxmi Devindrappa [38] studied the effects of heat transfer on the peristaltic MHD flow of a Bingham fluid through a porous medium in a channel. Rathod and Pallavi Kulkarni [39] investigated about the influence of wall properties on peristaltic transport of dusty fluid through porous medium. Rathod and Asha, [40] considered the effect of couple stress fluid on peristaltic motion in a uniform and non-uniform annulus.

Most of the physiological fluids such as blood behave as a non-Newtonian fluid due to various suspensions present in them. There are many non-Newtonian models like, power-law model, yield stress power-law model, couple-stress model, micropolar model, viscoelastic model and so on. Viscoelasticity in human blood is mainly due to the elastic energy stored in the deformation of red blood corpuscles as it flows through blood vessels due to peristaltic pumping by heart. The part of energy gained by blood due to pumping by heart is stored in the elastic form and the remaining is dissipated by viscosity. Earlier models which treated blood as a purely viscous fluid were inadequate as blood is a colloidal suspension of elastic red blood corpuscles. With this view point it is appropriate to consider a viscoelastic model to describe the behavior of blood. Based on relaxation and retardation times there are many viscoleastic fluid models like Maxwell model, Kelvin-Voigt model, Oldroid model, Jeffrey model and so on. The Jeffery fluid model is most used model due to its relevance to the study of peristaltic motion of blood. There are many works in literature concerning peristaltic flow of Jeffery fluid, some of the important ones are: Nadeem and Akbar [41] studied peristaltic flow of a Jeffrey fluid through an asymmetric channel by considering the viscosity to vary with temperature in accordance with Reynolds model. They assumed the fluid viscosity to vary as an exponential function of temperature. Mahmoud *et al.*, [42] investigated the combined effect of porous medium and magnetic field on peristaltic transport of a Jeffrey fluid and showed that both porous and magnetic parameters have retarding effect on the peristaltic flow. Rajanikanth *et al.*, [43] analyzed MHD peristaltic flow of a Jeffrey fluid in an asymmetric channel with partial slip and reported that the size of the bolus decreases with increasing Hartmann number and Jeffrey material parameter. Akbar *et al.*, [44] considered the Jeffrey fluid model for the study of peristaltic flow of chyme in the small intestine and presented exact solutions governing the flow characteristics. The study of nanoparticles concentration for the Jeffrey fluid model is considered by Nadeem *et al.*, [45] to study peristalsis in a three-dimensional rectangular channel having complaint walls and solved the same by homotopy perturbation technique. Nadeem *et al.*, [46] gave a mathematical model governing the peristaltic flow of Jeffrey fluid with nanoparticles phenomenon through a rectangular duct and showed that the presence of nano-sized particles in Jeffery fluid assists the peristaltic flow. Naga Jyothi *et al.*, [47] studied the effect of high frequency inlet and outlet pressure on the unsteady peristaltic flow of a Jeffrey fluid in a uniform converging tube. Riaz *et al.*, [48] obtained exact solution for the peristaltic flow of Jeffrey fluid in a three dimensional rectangular duct having slip at the walls and showed that Jeffrey fluid parameter increases the axial velocity while the slip parameter reduce the same. Al-Khafajy investigated the effects of wall properties and heat transfer on the peristaltic transport of a Jeffrey fluid through a channel filled with porous medium and reported that the Jeffrey parameter results in increase of velocity distribution and the size of the trapped Bolus and that the rigidity and stiffness play significant role in controlling the dynamics of the problem. El-dabe *et al.*, [49] obtained analytical solution for the peristaltic flow of a Jeffrey nanofluid in a tapered artery with mild stenosis and slip condition and found that the trapped bolus increases in size with the increase of both the maximum height of stenosis and the taper angle. Santhosh *et al.*, [50] analyzed the flow of a Jeffrey fluid through a porous medium in narrow tubes and showed that for given values of Jeffrey parameter, Darcy number and tube hematocrit, the effective viscosity increases with tube radius. Further, they showed that the core hematocrit and the mean hematocrit are respectively, decreasing and increasing functions of tube radius.

Majumder *et al.*, [51] showed that nanofluidic flow usually exhibits partial slip against the solid surface, which can be characterized by the so-called slip length, which varies in the range 3.4 – 68mm for different liquids. This implies that the slip conditions are the more realistic boundary conditions than the usual no slip boundary conditions. Several authors have considered effect of slip on the peristaltic flow in channels/tubes, see for example, Ebaid [19], Shob [20], Das [25] and Akbar *et al.*, [33]. Works of Rajanikanth *et al.*, [43], Riaz *et al.*, [48] and El-dabe *et al.*, [50] concern slip effects on the peristaltic flow of Jeffrey fluid. Recently, Akbar and Nadeem [53] considered both thermal and velocity slip effects on the peristaltic flow of a six constant Jeffrey's fluid model. Ebaid and Aly [54] and that of Rathod and Sanjeevkumar [55] have obtained closed form solutions for peristaltic flow of a nanofluid subjectd to partial slip conditions, without and with magnetic field effect, respectively.

In this paper the peristaltic flow of Jeffrey fluid with immersed nanoparticles in an asymmetric channel with flexible walls is proposed to be investigated. The contributions of nanoparticles are modeled through thermophoresis and Brownian diffusion effects. Closed form solutions are obtained for the equations that govern the conservations of momentum, heat and mass transports in the proposed problem.

2. MATHEMATICAL MODEL

We consider the two dimensional peristaltic transport of an incompressible Jeffrey fluid with suspended nanoparticles in an asymmetric channel with flexible walls, generated by propagation of waves on the channel walls travelling with different amplitudes and phases but with the same constant speed c. In the cartesian coordinate system (x, y), the left wall H_2 and the right wall H_1 are given by (see Figure 1).

$$H_1 = d_1 + a_1 \cos\left[\frac{2\pi}{\lambda}(x - ct)\right], \tag{1}$$

$$H_2 = -d_2 - b_1 \cos\left[\frac{2\pi}{\lambda}(x - ct) + \varphi\right]. \tag{2}$$

Here, a_1 and a_2 are the amplitudes of the waves, λ is the wave length, $d_1 + d_2$ is the width of the channel, φ is the phase difference with the range $0 \leq \varphi < \pi$, where $\varphi = 0$ and $\varphi = \pi$ corresponds to symmetric channel with waves out of the phase and in the phase, respectively. It should be noted that the following condition must be achieved

$$a_1^2 + b_1^2 + a_1 b_1 \cos\varphi \leq (d_1 + d_2)^2, \tag{3}$$

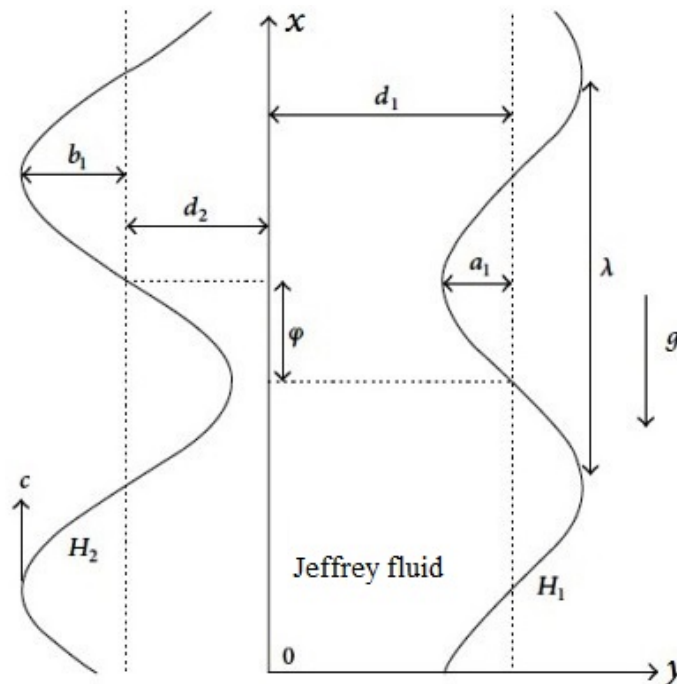with the choice of a_1, b_1, d_1, d_2 and φ, so that the walls will not intersect with each other.

Figure-1: Schematic of the flow configuration

The conservation equations governing the flow are of the form:

$$\nabla \cdot \mathbf{q} = 0, \tag{4}$$

$$\rho_f \left(\frac{\partial \mathbf{q}}{\partial t} + \mathbf{q} \cdot \nabla \mathbf{q} \right) = -\nabla p + div\ \boldsymbol{\tau} - \rho_f \left[\alpha \left(T - T_0 \right) + \alpha^* \left(S - S_0 \right) \right] \mathbf{g}, \tag{5}$$

$$(\rho C)_f \left(\frac{\partial T}{\partial t} + \mathbf{q} \cdot \nabla T \right) = k \nabla^2 T + (\rho C)_s \left[\left(\frac{D_T}{T_0} \right) \nabla T \nabla T + D_B \nabla S \nabla T \right] + q_1 \left(T - T_0 \right), \tag{6}$$

$$\frac{\partial S}{\partial t} + \mathbf{q} \cdot \nabla S = D_B \nabla^2 S + \left(\frac{D_T}{T_0} \right) \nabla^2 T, \tag{7}$$

where $\mathbf{q} = (u, v, 0)$ is the velocity vector, u and v are the velocities in x and y directions respectively, p is the pressure, $\mathbf{g} = (-g, 0, 0)$ is gravity vector, ∇^2 is the Laplacian operator, t is the time, ρ_f is the density of the fluid, ρ_s is the density of the nanoparticles, T is the temperature of the fluid, S is the nanoparticle concentration, k is the thermal conductivity, α and α^* are respectively the coefficients of thermal and solutal expansions, q_1 is coefficient of heat generation/absorption, C_f and C_s are respectively the specific heats at constant pressure of fluid and nanoparticles, T_0 and S_0 are the reference temperature and concentration, D_B is the Brownian diffusion coefficient, and D_T is the thermophoretic diffusion coefficient.

The constitutive relation for the stress tensor $\boldsymbol{\tau}$ for the Jeffrey fluid is given by

$$\boldsymbol{\tau} = \frac{\mu_f}{1 + \lambda_1} \left(\dot{\gamma} + \lambda_2 \frac{d\dot{\gamma}}{dt} \right), \tag{8}$$

where μ_f is the dynamic viscosity coefficient, λ_1 is the ratio of relaxation to retardation times, λ_2 is the retardation time, $\dot{\gamma}$ is the shear rate, $\frac{d}{dt}(\bullet) = \left(\frac{\partial}{\partial t} + \mathbf{q} \cdot \nabla \right)(\bullet)$ is the material derivative. The governing equations in component form are given by

$$\frac{\partial u}{\partial x} + \frac{\partial v}{\partial y} = 0, \tag{9}$$

$$\rho_f \left(\frac{\partial u}{\partial t} + u \frac{\partial u}{\partial x} + v \frac{\partial u}{\partial y} \right) = -\frac{\partial p}{\partial x} + \left(\frac{\partial \tau_{xx}}{\partial x} + \frac{\partial \tau_{xy}}{\partial y} \right) + \rho_f \left[\alpha \left(T - T_0 \right) + \alpha^* \left(S - S_0 \right) \right] g, \tag{10}$$

$$\rho_f \left(\frac{\partial v}{\partial t} + u \frac{\partial v}{\partial x} + v \frac{\partial v}{\partial y} \right) = -\frac{\partial p}{\partial y} + \left(\frac{\partial \tau_{yx}}{\partial x} + \frac{\partial \tau_{yy}}{\partial y} \right), \tag{11}$$

$$\frac{\partial T}{\partial t} + u \frac{\partial T}{\partial x} + v \frac{\partial T}{\partial y} = \frac{k}{(\rho C)_f} \left(\frac{\partial^2 T}{\partial x^2} + \frac{\partial^2 T}{\partial y^2} \right) + \frac{(\rho C)_s}{(\rho C)_f} \left[\frac{D_T}{T_0} \left(\frac{\partial T}{\partial y} \right)^2 + D_B \frac{\partial S}{\partial y} \frac{\partial T}{\partial y} \right] + q_1 \left(T - T_0 \right), \tag{12}$$

$$\frac{\partial S}{\partial t} + u \frac{\partial S}{\partial x} + v \frac{\partial S}{\partial y} = D_B \left(\frac{\partial^2 S}{\partial x^2} + \frac{\partial^2 S}{\partial y^2} \right) + \frac{D_T}{T_0} \left(\frac{\partial^2 T}{\partial x^2} + \frac{\partial^2 T}{\partial y^2} \right), \tag{13}$$

The stress components appearing in equations (10) and (11) are given by

$$\tau_{xx} = \frac{\mu_f}{1 + \lambda_1} \left[2 \frac{\partial u}{\partial x} + \lambda_2 \left(\frac{\partial}{\partial t} + u \frac{\partial}{\partial x} + v \frac{\partial}{\partial y} \right) \left(2 \frac{\partial u}{\partial x} \right) \right], \tag{14}$$

$$\tau_{xy} = \tau_{yx} = \frac{\mu_f}{1 + \lambda_1} \left[\left(\frac{\partial u}{\partial y} + \frac{\partial v}{\partial x} \right) + \lambda_2 \left(\frac{\partial}{\partial t} + u \frac{\partial}{\partial x} + v \frac{\partial}{\partial y} \right) \left(\frac{\partial u}{\partial y} + \frac{\partial v}{\partial x} \right) \right], \tag{15}$$

$$\tau_{yy} = \frac{\mu_f}{1 + \lambda_1} \left[2 \frac{\partial v}{\partial y} + \lambda_2 \left(\frac{\partial}{\partial t} + u \frac{\partial}{\partial x} + v \frac{\partial}{\partial y} \right) \left(2 \frac{\partial v}{\partial y} \right) \right]. \tag{16}$$

Following Shapiro *et al.*, [3] we introduce a wave frame of reference (X,Y) moving with velocity c in which the motion becomes independent of time when the channel is an integral multiple of the wavelength and the pressure difference at the ends of the channel is a constant. The transformation from fixed frame of reference (x, y) to the wave frame of reference (X,Y) is given by

$$X = x - ct, \quad Y = y, \quad U = u - c, \quad V = v, \quad W = \omega, \quad P(X,Y) = p(x, y, t), \tag{17}$$

where (U,V) are the velocities along coordinate axes in the wave frame and (u,v) are those in the fixed frame of reference, W is the angular velocity in the wave frame and ω is the angular velocity in the fixed frame of reference. The pressure $P(X,Y)$ remains a constant across any axial station of the channel under the assumption that the wavelength is large and the curvature effects are negligible. We now use the nondimensional variables defined by:

$$
\begin{aligned}
& x^* = \frac{2\pi}{\lambda} X, \quad y^* = \frac{Y}{d_1}, \quad u^* = \frac{U}{c}, \quad v^* = \frac{V}{\delta c}, \quad \delta = \frac{2\pi d_1}{\lambda}, \quad p^* = \frac{\delta d_1}{\mu_f c} P, \\
& \tau_{x^* x^*} = \frac{d_1 \tau_{XX}}{\mu_f c}, \quad \tau_{x^* y^*} = \frac{d_1 \tau_{XY}}{\mu_f c}, \quad \tau_{y^* x^*} = \frac{d_1 \tau_{YX}}{\mu_f c}, \quad \tau_{y^* y^*} = \frac{d_1 \tau_{YY}}{\mu_f c}, \\
& h_1 = \frac{H_1}{d_1}, \quad h_2 = \frac{H_2}{d_1}, \quad d = \frac{d_2}{d_1}, \quad a = \frac{a_1}{d_1}, \quad b = \frac{b_1}{d_1}, \quad \theta = \frac{T - T_0}{T_1 - T_0}, \quad \phi = \frac{S - S_0}{S_1 - S_0}.
\end{aligned}
\tag{18}
$$

Substituting for new variables from (17) and (18) in equations (9) – (16) and dropping asterisks for simplicity, we get the following equations in the nondimensional form

$$\frac{\partial u}{\partial x} + \frac{\partial v}{\partial y} = 0, \tag{19}$$

$$\delta \operatorname{Re}\left(u \frac{\partial u}{\partial x} + v \frac{\partial u}{\partial y}\right) = -\frac{\partial p}{\partial x} + \left(\delta \frac{\partial \tau_{xx}}{\partial x} + \frac{\partial \tau_{xy}}{\partial y}\right) + Gr\theta + Gr^*\phi, \tag{20}$$

$$\delta^3 \operatorname{Re}\left(u \frac{\partial v}{\partial x} + v \frac{\partial v}{\partial y}\right) = -\frac{\partial p}{\partial y} + \left(\delta^2 \frac{\partial \tau_{yx}}{\partial x} + \delta \frac{\partial \tau_{yy}}{\partial y}\right), \tag{21}$$

$$\delta \operatorname{Pr} \operatorname{Re}\left(u \frac{\partial \theta}{\partial x} + v \frac{\partial \theta}{\partial y}\right) = \delta^2 \frac{\partial^2 \theta}{\partial x^2} + \frac{\partial^2 \theta}{\partial y^2} + Nt\left(\frac{\partial \theta}{\partial y}\right)^2 + Nb \frac{\partial \phi}{\partial y} \frac{\partial \theta}{\partial y} + Q_1\theta, \tag{22}$$

$$\delta Sc \operatorname{Re}\left(u \frac{\partial \phi}{\partial x} + v \frac{\partial \phi}{\partial y}\right) = \delta^2 \frac{\partial^2 \phi}{\partial x^2} + \frac{\partial^2 \phi}{\partial y^2} + \frac{Nt}{Nb}\left(\delta^2 \frac{\partial^2 \theta}{\partial x^2} + \frac{\partial^2 \theta}{\partial y^2}\right), \tag{23}$$

$$\tau_{xx} = \frac{2\delta}{1+\lambda_1}\left[\frac{\partial u}{\partial x} + \lambda_2\left(\frac{c\delta}{d_1}\right)\left(u \frac{\partial}{\partial x} + v \frac{\partial}{\partial y}\right)\left(\frac{\partial u}{\partial x}\right)\right], \tag{24}$$

$$\tau_{xy} = \tau_{yx} = \frac{2}{1+\lambda_1}\left[\left(\frac{\partial u}{\partial y} + \delta^2 \frac{\partial v}{\partial x}\right) + \lambda_2\left(\frac{c\delta}{d_1}\right)\left(u \frac{\partial}{\partial x} + v \frac{\partial}{\partial y}\right)\left(\frac{\partial u}{\partial y} + \delta^2 \frac{\partial v}{\partial x}\right)\right], \tag{25}$$

$$\tau_{yy} = \frac{2\delta}{1+\lambda_1}\left[\frac{\partial v}{\partial y} + \lambda_2\left(\frac{c\delta}{d_1}\right)\left(u \frac{\partial}{\partial x} + v \frac{\partial}{\partial y}\right)\left(\frac{\partial v}{\partial y}\right)\right], \tag{26}$$

The nondimensional parameters appearing in equations (20) – (23) are:

$$\operatorname{Re} = \frac{cd_1}{\upsilon_f} \qquad \text{the Reynolds number}$$

$$Gr = \frac{\rho_f \alpha g (T_1 - T_0) d_1^2}{\mu_f c} \qquad \text{the thermal Grashof number}$$

$$Gr^* = \frac{\rho_f \alpha^* g (S_1 - S_0) d_1^2}{\mu_f c} \qquad \text{the solutal Grashof number}$$

$$\Pr = \frac{(\mu C)_f}{k} \qquad \text{the Prandtl number}$$

$$Sc = \frac{\upsilon_f}{D_B} \qquad \text{the Schmidt number}$$

$$Nt = \frac{(\rho C)_s D_T (T_1 - T_0)}{k T_0} \qquad \text{the thermophoresis parameter}$$

$$Nb = \frac{(\rho C)_s D_B (S_1 - S_0)}{k} \qquad \text{the Brownian motion parameter}$$

$$Q_1 = \frac{q_1 (\rho c)_f d_1^2}{k} \qquad \text{the heat source/sink parameter}$$

Using stream function $\psi(x, y)$ defined by

$$u = \frac{\partial \psi}{\partial y}, \quad v = -\frac{\partial \psi}{\partial x},$$

the continuity equation (19) is identically satisfied and the equations (20) – (26), together with long wave length approximation ($\delta \ll 1$) and low Reynolds number limit ($\mathrm{Re} \ll 1$), take the form:

$$\frac{\partial p}{\partial x} = \frac{1}{1 + \lambda_1} \frac{\partial^3 \psi}{\partial y^3} + Gr\theta + Gr^* \phi, \tag{27}$$

$$\frac{\partial p}{\partial y} = 0, \tag{28}$$

$$\frac{\partial^2 \theta}{\partial y^2} + Nb \frac{\partial \theta}{\partial y} \frac{\partial \phi}{\partial y} + Nt \left(\frac{\partial \theta}{\partial y} \right)^2 + Q_1 \theta = 0, \tag{29}$$

$$\frac{\partial^2 \phi}{\partial y^2} + \frac{Nt}{Nb} \frac{\partial^2 \theta}{\partial y^2} = 0. \tag{30}$$

Eliminating pressure from equations (27) and (28) we get

$$\frac{1}{1 + \lambda_1} \frac{\partial^4 \psi}{\partial y^4} + Gr \frac{\partial \theta}{\partial y} + Gr^* \frac{\partial \phi}{\partial y} = 0. \tag{31}$$

In solving equations (29) – (31) we make use of the following boundary conditions:

$$\psi = \frac{F}{2}, \quad \frac{\partial \psi}{\partial y} + \beta \frac{\partial^2 \psi}{\partial y^2} = -1 \quad \text{at} \quad y = h_1 = 1 + a \cos x \tag{32}$$

$$\psi = \frac{-F}{2}, \quad \frac{\partial \psi}{\partial y} - \beta \frac{\partial^2 \psi}{\partial y^2} = -1 \quad \text{at} \quad y = h_2 = -d - b \cos(x + \varphi) \tag{33}$$

$$\theta + Bi \frac{\partial \theta}{\partial y} = 0, \quad \phi + Bi^* \frac{\partial \phi}{\partial y} = 0 \quad \text{at} \quad y = h_1 \tag{34}$$

$$\theta - Bi \frac{\partial \theta}{\partial y} = 1, \quad \phi - Bi^* \frac{\partial \phi}{\partial y} = 1 \quad \text{at} \quad y = h_2 \tag{35}$$

where F is dimensionless time-mean flow in the wave frame to be defined in the next section, β is the slip parameter, Bi and Bi^* are thermal and solutal Biot numbers respectively.

2.1 Rate of volume flow

The instantaneous volume flow rate in the fixed frame is given by

$$q(x,t) = \int_{H_2}^{H_1} u(x,y,t)\,dy \tag{36}$$

where H_1 and H_2 are given by equations (1) and (2) respectively. The rate of volume flow in the wave frame is given by

$$q^*(X) = \int_{H_2}^{H_1} U(X,Y)\,dY \tag{37}$$

where $H_1 = H_1(X)$ and $H_2 = H_2(X)$ are functions of X alone. If we substitute (17) into (36) and make use of (37), we find that the two rates of volume flow are related through

$$q(x,t) = q^*(X) + c\left[H_1(x,t) - H_2(x,t)\right] \tag{38}$$

The time-mean flow over a period T at a fixed position x is defined as

$$q(x) = \frac{1}{T}\int_0^T q(x,t)\,d \tag{39}$$

where, $T = \dfrac{\lambda}{c}$ is the period of the wave. Now integrating (38) with respect to t over a wave period and using (39) yields the following equation

$$q(x) = q^*(X) + c(d_1 + d_2) \tag{40}$$

On defining the dimensionless time-mean flows Q and F, respectively, in the fixed and wave frame as

$$Q = \frac{q}{d_1 c}, \quad F = \frac{q^*}{d_1 c}$$

One finds that equation (40) may be written as

$$Q = F + 1 + d \tag{41}$$

where $F = \displaystyle\int_{h_2}^{h_1} \frac{\partial \psi}{\partial y}\,dy = \psi(h_1) - \psi(h_2)$. This is made use in defining the boundary conditions on velocity.

2.2 Pressure rise per wavelength

When the flow is steady in the wave frame, one can characterize the pumping performance by means of the pressure rise per wavelength. The nondimensional pressure rise per wavelength in the wave frame are defined as

$$\Delta P_\lambda = \int_{h_2}^{h_1} \left(\int_0^\lambda \frac{\partial p}{\partial x}\,dx\right) dy \tag{42}$$

In sections to follow, we present the closed form solutions for the energy, species and linear and angular momentum conservation equations, respectively.

3. CLOSED FORM SOLUTIONS OF ENERGY AND SPECIES EQUATIONS

In this section the closed form solutions of the equations (29) – (30) subjected to the boundary conditions (34) – (35) are presented. Integrating equation (30) with respect to y once can get

$$\frac{\partial \phi}{\partial y} = -\frac{Nt}{Nb}\frac{\partial \theta}{\partial y} + f_1(x). \tag{43}$$

Substituting equation (43) in equation (30) the following second order differential equation in θ is obtained:

$$\frac{\partial^2 \theta}{\partial y^2} + Nbf_1(x)\frac{\partial \theta}{\partial y} + Q_1\theta = 0. \tag{44}$$

The solution of the above equation can be obtained as

$$\theta(x, y) = f_2(x)e^{m_1 y} + f_3(x)e^{m_2 y}. \tag{45}$$

Here, $m_1 = \frac{1}{2}\left\{-Nbf_1(x) + \sqrt{Nb^2 f_1^2(x) - 4Q_1}\right\}$ and $m_2 = \frac{1}{2}\left\{-Nbf_1(x) - \sqrt{Nb^2 f_1^2(x) - 4Q_1}\right\}$.

Using the solution (45) in equation (43) and integrating with respect to y, the solution of equation (43) can be written as

$$\phi(x, y) = -\frac{Nt}{Nb}\left\{f_2(x)e^{m_1 y} + f_3(x)e^{m_2 y}\right\} + f_1(x)y + f_4(x). \tag{46}$$

In equations (45) and (46) f_i, $i = 1, 2, 3, 4$ represent arbitrary functions of x that are to be determined. Using boundary conditions (34) and (35) we get the following relations for f_2, f_3 and f_4 in terms of f_1:

$$f_2 = \frac{1}{(1 - m_1 Bi)(1 + m_2 Bi)e^{m_1 h_2 + m_2 h_1} - (1 + m_1 Bi)(1 - m_2 Bi)e^{m_1 h_1 + m_2 h_2}}, \tag{47}$$

$$f_3 = -\left(\frac{1 + m_1 Bi}{1 + m_2 Bi}\right)\frac{e^{m_1 h_1 - m_2 h_1}}{(1 - m_1 Bi)(1 + m_2 Bi)e^{m_1 h_2 + m_2 h_1} - (1 + m_1 Bi)(1 - m_2 Bi)e^{m_1 h_1 + m_2 h_2}}, \tag{48}$$

$$f_4 = \frac{Nt}{Nb}\left\{(1 + m_1 Bi^*)f_2 e^{m_1 h_1} + (1 + m_2 Bi^*)f_3 e^{m_2 h_1}\right\} - \left(h_1 + Bi^*\right)f_1, \tag{49}$$

where f_1 satisfies the implicit relation

$$\frac{\frac{Nt}{Nb}\left[(1 - m_1 Bi^*)e^{m_1 h_2} - (1 + m_1 Bi^*)e^{m_1 h_1} - \left(\frac{1 + m_1 Bi}{1 + m_2 Bi}\right)\frac{e^{m_1 h_1}}{e^{m_2 h_2}}\left\{(1 - m_2 Bi^*)e^{m_2 h_2} - (1 + m_2 Bi^*)e^{m_2 h_1}\right\}\right]}{(1 - m_1 Bi)(1 + m_2 Bi)e^{m_1 h_2 + m_2 h_1} - (1 + m_1 Bi)(1 - m_2 Bi)e^{m_1 h_1 + m_2 h_2}} \tag{50}$$
$$+ \left(h_1 - h_2 + 2Bi^*\right)f_1 + 1 = 0$$

4. SOLUTION OF MOMENTUM EQUATION

On using the solutions (45) and (46) in equation (31) the solution for stream function $\psi(x, y)$ can be obtained in the form

$$\psi(x, y) = g_1(x)\frac{y^3}{6} + g_2(x)\frac{y^3}{2} + g_3(x)y + g_4(x) - (1 + \lambda_1)Gr^* f_1 \frac{y^4}{24} \tag{51}$$
$$- (1 + \lambda_1)\widetilde{Gr}\left\{\frac{f_2(x)}{m_1^3}e^{m_1 y} + \frac{f_3(x)}{m_2^3}e^{m_2 y}\right\}$$

Here, $\widetilde{Gr} = Gr - \frac{Nt}{Nb}Gr^*$. The arbitrary functions $g_i(x)$, $i = 1, 2, 3, 4$, on using boundary conditions (32) and (33), can be obtained from the matrix system:

$$
\begin{bmatrix}
\dfrac{h_1^3}{6} & \dfrac{h_1^2}{2} & h_1 & 1 \\[2ex]
\dfrac{h_2^3}{6} & \dfrac{h_2^2}{2} & h_2 & 1 \\[2ex]
\left(\dfrac{h_1}{2}+\beta\right)h_1 & h_1+\beta & 1 & 0 \\[2ex]
\left(\dfrac{h_2}{2}-\beta\right)h_2 & h_2-\beta & 1 & 0
\end{bmatrix}
\begin{bmatrix}
g_1(x) \\ g_2(x) \\ g_3(x) \\ g_4(x)
\end{bmatrix}
=
\begin{bmatrix}
c_1 \\ c_2 \\ c_3 \\ c_4
\end{bmatrix},
\tag{52}
$$

where,

$$
c_1 = \frac{F}{2} + (1+\lambda_1)\widetilde{Gr}\left\{\frac{f_2}{m_1^3}e^{m_1 h_1} + \frac{f_3}{m_2^3}e^{m_2 h_1}\right\} + (1+\lambda_1)Gr^* f_1 \frac{h_1^4}{24},
$$

$$
c_2 = \frac{-F}{2} + (1+\lambda_1)\widetilde{Gr}\left\{\frac{f_2}{m_1^3}e^{m_1 h_2} + \frac{f_3}{m_2^3}e^{m_2 h_2}\right\} + (1+\lambda_1)Gr^* f_1 \frac{h_2^4}{24},
$$

$$
c_3 = (1+\lambda_1)\widetilde{Gr}\left\{\frac{f_2}{m_1^2}(1+m_1\beta)e^{m_1 h_1} + \frac{f_3}{m_2^2}(1+m_2\beta)e^{m_2 h_1}\right\} + (1+\lambda_1)Gr^* f_1 \frac{h_1^2}{2}\left(\frac{h_1}{3}+\beta\right) - 1,
$$

$$
c_4 = (1+\lambda_1)\widetilde{Gr}\left\{\frac{f_2}{m_1^2}(1-m_1\beta)e^{m_1 h_2} + \frac{f_3}{m_2^2}(1-m_2\beta)e^{m_2 h_2}\right\} + (1+\lambda_1)Gr^* f_1 \frac{h_2^2}{2}\left(\frac{h_2}{3}-\beta\right) - 1,
$$

In the following section the discussion of the results obtained with the help of analytical and approximate analytical solutions obtained so far, is presented.

5. RESULTS AND DISCUSSION

In this section the discussion of some important results obtained through the exact solutions for the velocity, temperature, nanoparticle distributions and pressure rise over a wavelength are presented. It is to be noted that the effect of geometry on the peristaltic flow has already been extensively reported in the literature; hence the results pertaining to the important physical parameters like Jeffrey parameter, heat source/sink parameter, Biot numbers and nanoparticle parameters are only presented. Also, from equations (27) - (30) it can be noted that the momentum, energy and species conservation equations are partially decoupled. This means that the Jeffrey parameter affect velocity alone and have no effect on the temperature and nanoparticle concentrations. But the parameters that affect temperature and concentration of nanoparticles may have some effect on the velocity distribution. In studying the effect of individual parameters we fix the values of the other parameters as follows: $a = 0.1$, $b = 0.5$, $d = 1$, $x = 1$, $\varphi = 0.2$, $Nt = 1$, $Nb = 0.8$, $Bi = Bi^* = 0.5$, $F = 5$, $\beta = 0.5$, $Gr = 1$, $Gr^* = 0.5$, $\lambda_1 = 0.5$ and $Q_1 = -2$. At this juncture it is to be mentioned that the solutions for velocity, temperature and nanoparticle concentration distributions depend on the arbitrary functions $f_i(x)$, $i = 1, 2, 3, 4$ and $g_i(x)$, $i = 1, 2, 3, 4$. The value of the function f_1, for a particular combination of parameter values, is obtained from the implicit relation (50) using Newton – Raphson scheme. Values of other functions can be obtained from equations (47) – (49), and the linear system (52).

Figure 2 highlights the effect of Jeffrey parameter λ_1 on the velocity distribution $u(y)$ in the presence and absence of nanoparticles. It is to be noted that in the absence of nanoparticles, i.e., $Nt \approx 0$ and $Nb \approx 0$, the velocity, in almost left half of the channel, increases for increasing values of Jeffery parameter λ_1 while the opposite is true in the right half plane. The velocity profile remains parabolic and the maximum velocity shifts towards the left wall with the increase in the values of Jeffrey parameter λ_1. There is a point in the channel near $y = -0.25$, where the velocity is independent of Jeffrey parameter, that is, any variations in the Jeffrey parameter will not affect the velocity at that point. The said results in case of peristaltic flow of clear Jeffery fluid hold good qualitatively in the case of peristaltic flow of Jeffrey fluid with nanoparticles suspensions, i.e., $Nt \neq 0$ and $Nb \neq 0$, except that the velocity is less in the left half plane and more in the right half plane of the channel, in comparison with the clear fluid case.
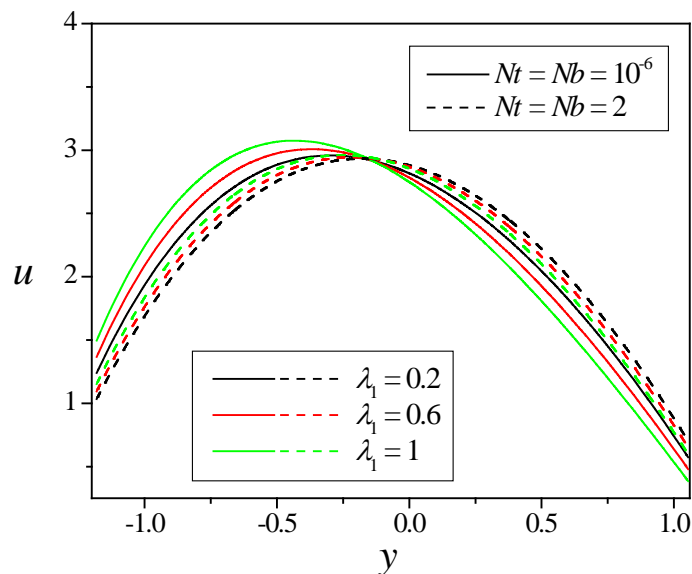
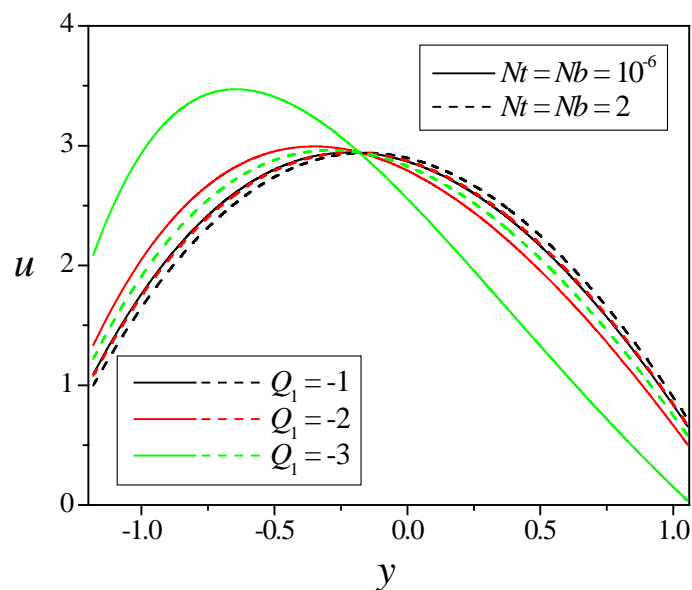**Figure-2:** Velocity distribution for different values of Jeffrey parameter

Figure-3: Velocity distribution for different values of heat source/sink parameter

Figure 3 shows the variation of velocity distribution $u(y)$ with respect to heat source/sink parameter Q_1. It should be noted that $Q_1 > 0$ corresponds to heat generation and $Q_1 < 0$ corresponds to heat absorption. From figure 3 one can notice that, in the absence of nanoparticles, i.e., $Nt \approx 0$ and $Nb \approx 0$, the velocity is the left half the channel is an increasing function of $Q_1 < 0$ while the opposite holds in the right half of the channel. As observed in case of λ_1 there exist a stagnation point near $y = -0.25$, where the velocity is independent of heat source/sink parameter. The results are qualitatively same in the presence of nanoparticles $Nt \neq 0$ and $Nb \neq 0$.
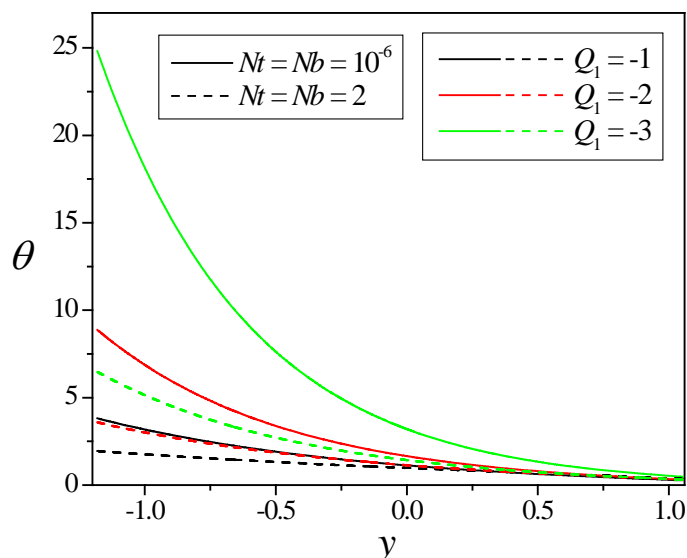
Figure-4: Temperature distribution for different values of heat source/sink parameter

Figure 4 depicts the variation of temperature distribution with respect to heat source/sink parameter for different values of Nt and Nb. From, figure 4 one can make out that, in the case of clear fluid, i.e., $Nt \approx 0$ and $Nb \approx 0$, for a given value of Q_1 the temperature decays from a higher value at the left wall to a lower value at the right wall. Increasing negative values of Q_1 results in increasing the temperature in the channel, which is quite unrealistic as the presence of heat sink one expects the temperature to decrease. This may be due to the fact that two-way coupling between the energy and species conservation equations and the robin type of boundary conditions. This creates a peculiar environment where in the heat sink ($Q_1 < 0$) instead of annihilating heat adds heat to the system. These results agree qualitatively in case of Jeffrey fluid with suspended nanoparticles, i.e., $Nt \neq 0$ and $Nb \neq 0$.

Figure 5 projects the variation of nanoparticle distribution heat source/sink parameter Q_1 for different values of Nt and Nb. From, figure 5 it is clear the nanoparticle concentration is a decreasing function of heat source/sink parameter Q_1 in the absence ($Nt \approx 0$ and $Nb \approx 0$) and in the presence of ($Nt \neq 0$ and $Nb \neq 0$) nanoparticle suspensions. . For a given for a given value of Q_1 the nanoparticle concentration increases from lower value at the left wall to a higher value at the right wall.
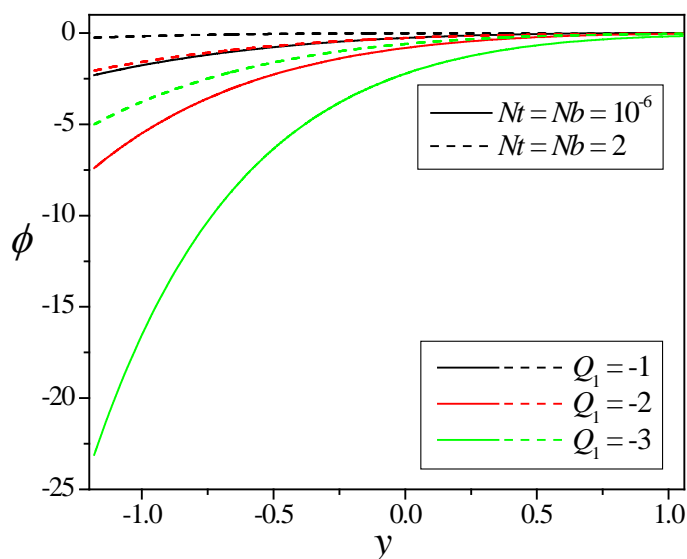

Figure-5: Concentration distribution for different values of heat source/sink parameter

The results pertaining to variation of Biot numbers Bi and Bi^*, Grashof numbers Gr and Gr^* and the slip parameter β, are qualitatively similar to that observed in the Newtonian case. Hence discussions of the same are omitted here. We now present the effect of Jeffrey and heat source/sink parameters on the pressure rise over a wavelength. Figure 6 indicates the variation of the pressure rise ΔP_λ per wavelength against the time averaged flux Q for different values of Jeffrey parameter λ_1. The time averaged flux Q corresponding to the zero pressure rise, i.e., $\Delta P_\lambda = 0$, which is the case of free pumping, is denoted by Q^*. The following four sub-regions of the graph are considered,

(i) $\Delta P_\lambda = 0$ and $Q = Q^*$ – the free pumping region,

(ii) $\Delta P_\lambda > 0$ and $Q < 0$ – the backward pumping region,

(iii) $\Delta P_\lambda > 0$ and $Q < Q^*$ – the peristaltic pumping region and

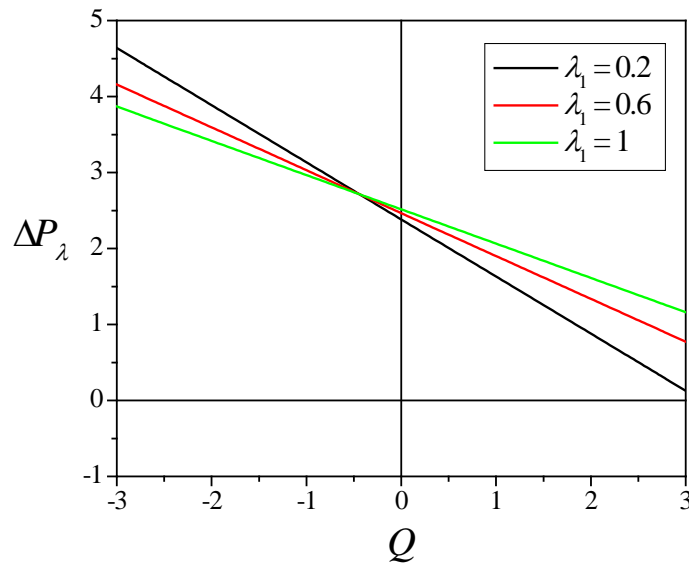(iv) $\Delta P_\lambda < 0$ and $Q > Q^*$ – the co-pumping region.

Figure-6: Pressure rise over a wavelength as a function of flow rate for different values of Jeffrey parameter

It has been observed that in the backward pumping region the pressure rise over a wavelength ΔP_λ decreases with increasing values of Jeffrey parameter λ_1, until the time averaged flow rate Q reaches a critical value $Q_c = -0.5$ and increases thereafter. It has been observed that inn the co-pumping region the pressure rise over a wavelength ΔP_λ increases with increasing values of Jeffrey parameter λ_1 but figure 6 domain is restricted to interval $-3 \le Q \le 3$. In the peristaltic pumping region the pressure rise over a wavelength ΔP_λ is an increasing function of the Jeffrey parameter λ_1. The increase in the pressure rise due to the non-Newtonian nature of the carrier fluid, in the peristaltic pumping region indicates that flow will be retarded. As a consequence of the retarded motion, the drug carrying nanoparticles can be concentrated near tumor and the drug will be effectively delivered at the required region facilitating the cure of carcinogenic tissue.

Figure 7 shows the effect of heat source/sink parameter Q_1 on the pressure rise over a wavelength ΔP_λ as a function of time averaged flux Q. From Figure 7 one can observe that the time average flow rate Q^* corresponding to free pumping, i.e., $\Delta P_\lambda = 0$ increases with increasing values of heat sink parameter ($Q_1 < 0$). Figure 7 indicates that in the backward pumping region the pressure rise over a wavelength ΔP_λ increases with increasing values of heat sink parameter. In the peristaltic pumping region the pressure rise over a wavelength ΔP_λ is an increasing function of the heat sink parameter Q_1 which retards the flow and creates conducive environment for an effect drug delivery.
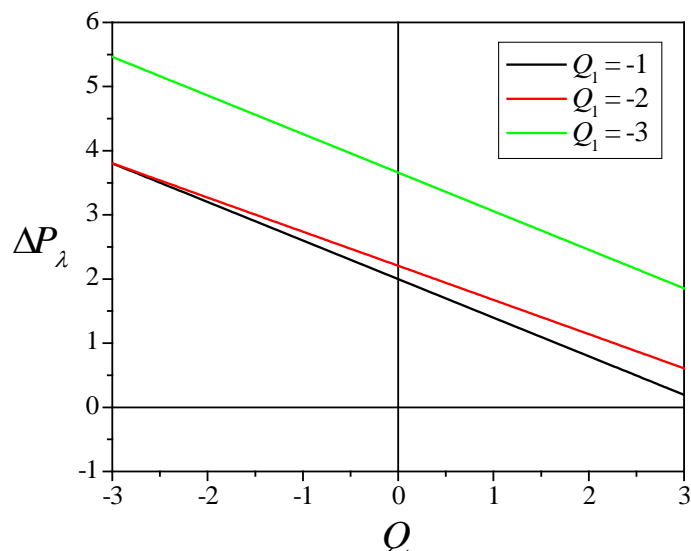
Figure-7: Pressure rise over a wavelength as a function of flow rate for different values of heat source/sink parameter

5. CONCLUSIONS

The exact solutions for equations governing conservation of momentum, heat and mass transport in the peristaltic flow of a Jeffrey fluid with immersed nanoparticles, through an asymmetric channel subject to general boundary conditions were obtained. Graphical representation of temperature distribution, nanoparticle distribution, velocity distribution and pressure rise over a wavelength for some chosen values of parameters were also presented. The following are few important results of the present analysis:

1. The Jeffrey parameter and the heat source/sink parameter have mixed behavior on the velocity profiles.
2. Heat sinks have got an adverse effect on the temperature distribution that is instead of removing heat from the fluid it adds heat.
3. The pressure rise in the peristaltic pumping region increases with Jeffrey parameter as well as the heat sink parameter.
4. Peristalsis of Jeffrey fluid with a heat sink can effectively be used for effective drug delivery and the cure of carcinoma.

REFERENCES

[1] T. W. Latham, *Fluid motion in a peristaltic pump* [M.S. thesis], MIT, Cambridge, UK, 1966.
[2] T.-F. Zien and S. Ostrach, "A long wave approximation to peristaltic motion," *Journal of Biomechanics*, vol. 3, no. 1, pp. 63–75, 1970.
[3] J.-S. Lee and Y.-C. Fung, "Flow in nonuniform small blood vessels," *Microvascular Research*, vol. 3, no. 3, pp. 272–287, 1971.
[4] P. Chaturani and V. P. Rathod, A theoretical model for pulsatile blood flow with applications to cerebrovascular diseases, Neurological Research 3 (1981) 289 –303.
[5] L. M. Srivastava, V. P. Srivastava and S. N. Sinha, "Peristaltic transport of a physiological fluid. Part I. Flow in non-uniform geometry," *Biorheology*, vol. 20, no. 2, pp. 153–166, 1983.
[6] S. Takabatake, K. Ayukawa and A. Mori, "Peristaltic pumping in circular cylindrical tubes: a numerical study of fluid transport and its efficiency," *Journal of Fluid Mechanics*, vol. 193, pp. 267– 283, 1988.
[7] E. F. El Shehawey and K. S. Mekheimer, "Couple-stresses in peristaltic transport of fluids," *Journal of Physics D*, vol. 27, no. 6, pp. 1163–1170, 1994.
[8] R. A. Ramachandra and S. Usha, "Peristaltic transport of two immiscible viscous fluids in a circular tube," *Journal of Fluid Mechanics*, vol. 298, pp. 271–285, 1995.
[9] K. S. Mekheimer, "Peristaltic transport of a couple stress fluid in a uniform and non-uniform channels," *Biorheology*, vol. 39, no.6, pp. 755–765, 2002.
[10] J. C. Misra and S. K. Pandey, Peristaltic transport of blood in small vessels: Study of a mathematical model, Computers and Mathematics with Applications vol. 43, pp. 1183-1193, 2002.
[11] K. Vajravelu, S. Sreenadh and V. R. Babu, "Peristaltic transport of a Herschel-Bulkley fluid in an inclined tube," *International Journal of Non-Linear Mechanics*, vol. 40, no. 1, pp. 83–90, 2005.
[12] K. S. Mekheimer and Y. Abd Elmaboud, "The influence of heat transfer and magnetic field on peristaltic transport of a Newtonian fluid in a vertical annulus: application of an endoscope," *Physics Letters A*, vol. 372, no. 10, pp. 1657–1665, 2008.

[13] V. P. Rathod and S. Tanveer, Pulsatile flow of couple stress fluid through a porous medium with Periodic Body acceleration and magnetic Field, Bull. Malays. Math. Sci. Soc. 32 (2) (2009) 245–259.

[14] K. De Vries, E. A. Lyons, G. Ballard, C. S. Levi and D. J. Lindsay, "Contractions of the inner third of themyometrium," *American Journal of Obstetrics and Gynecology*, vol. 162, no. 3,pp. 679–682, 1990.

[15] A. Ramachandra Rao and M. Mishra, Nonlinear and curvature effects on peristaltic flow of a viscous fluid in an asymmetric channel, Acta Mechanica, 168 (2004), 35 - 59.

[16] E. F. Elshehawey, N. T. Eldabe, E. M. Elghazy, and A. Ebaid, "Peristaltic transport in an asymmetric channel through a porous medium," *Applied Mathematics and Computation*, vol. 182, no. 1, pp. 140–150, 2006.

[17] M. V. Subba Reddy, A. Ramachandra Rao, and S. Sreenadh, "Peristaltic motion of a power-law fluid in an asymmetric channel," *International Journal of Non-Linear Mechanics*, vol. 42, no. 10, pp. 1153–1161, 2007.

[18] N. Ali and T. Hayat, Peristaltic flow of a micropolar fluid in an asymmetric channel. Comput Math Appl, 55 (2008), 589-608.

[19] A. Ebaid, "Effects of magnetic field and wall slip conditions on the peristaltic transport of a Newtonian fluid in an asymmetric channel," *Physics LettersA*, vol. 372, no. 24, pp.4493–4499, 2008.

[20] A. M. Sobh, "Slip flow in peristaltic transport of a Carreau fluid in an asymmetric channel," *Canadian Journal of Physics*, vol. 87, no. 8, pp. 957–965, 2009.

[21] G. C. Shit, M. Roy and E. Y. K. Ng, "Effect of induced magnetic field on peristaltic flow of a micropolar fluid in an asymmetric channel," *International Journal for Numerical Methods in Biomedical Engineering*, vol. 26, no. 11, pp. 1380–1403, 2010.

[22] K. S. Mekheimer, S. Z. A. Husseny and Y. Abd Elmaboud, "Effects of heat transfer and space porosity on peristaltic flow in a vertical asymmetric channel," *Numerical Methods for Partial Differential Equations*, vol. 26, no. 4, pp. 747–770, 2010.

[23] S. Srinivas and R. Muthuraj, "Effects of chemical reaction and space porosity on MHD mixed convective flow in a vertical asymmetric channel with peristalsis," *Mathematical and Computer Modelling*, vol. 54, no. 5-6, pp. 1213–1227, 2011.

[24] S. Srinivas, R. Gayathri and M. Kothandapani, "Mixed convective heat and mass transfer in an asymmetric channel with peristalsis," *Communications in Nonlinear Science and Numerical Simulation*, vol. 16, no. 4, pp. 1845–1862, 2011.

[25] K. Das, "Influence of slip and heat transfer on MHD peristaltic flow of a Jeffrey fluid in an inclined asymmetric porous channel," *Indian Journal of Mathematics*, vol. 54, pp. 19–45, 2012.

[26] Y. Abd Elmaboud, S. Kh. Mekheimer, and A. I. Abdellateef, "Thermal properties of couple-stress fluid flow in an asymmetric channel with peristalsis," *Journal of Heat Transfer*, vol. 135, no. 4, 8 pages, 2013.

[27] Yeng-Yung Tsui, Da-Ching Guo, Shin-Hung Chen, Shi-Wen Lin, Pumping flow in a channel with a peristaltic wall, *ASME Journal of Fluids Engineering*, vol. 136, art. id. 021202, pp. 1-9, 2014.

[28] S. U. S. Choi, "Enhancing thermal conductivity of fluids with nanoparticles," in *The Proceedings of the ASME International Mechanical Engineering Congress and Exposition*, ASME, San Francisco, Calif, USA. Computational and Mathematical Methods in Medicine

[29] S. U. S. Choi, Z. G. Zhang, W. Yu, F. E. Lockwood, and E. A. Grulke, "Anomalous thermal conductivity enhancement in nanotube suspensions," *Applied Physics Letters*, vol. 79, no. 14, pp. 2252–2254, 2001.

[30] N. S. Akbar and S. Nadeem, "Endoscopic effects on peristaltic flow of a nanofluid," *Communications in Theoretical Physics*, vol. 56, no. 4, pp. 761–768, 2011.

[31] N. S. Akbar and S. Nadeem, "Peristaltic flow of a Phan-Thien-Tanner nanofluid in a diverging tube," *Heat Transfer*, vol. 41, no.1, pp. 10–22, 2012.

[32] N. S. Akbar, S. Nadeem, T. Hayat, and A. A. Hendi, "Peristaltic flow of a nanofluid in a non-uniform tube," *Heat and Mass Transfer/Waerme-und Stoffuebertragung*, vol. 48, no. 2, pp. 451– 459, 2012.

[33] N. S. Akbar, S. Nadeem, T. Hayat, and A. A. Hendi, "Peristaltic flow of a nanofluid with slip effects,"*Meccanica*, vol. 47,pp. 1283–1294, 2012.

[34] M. Mustafa, S. Hina, T. Hayat, and A. Alsaedi, "Influence of wall properties on the peristaltic flow of a nanofluid: analytic and numerical solutions," *International Journal of Heat and Mass Transfer*, vol. 55, pp. 4871 – 4877, 2012.

[35] O. A. Beg and D. Tripathi, "Mathematica simulation of peristaltic pumping with double-diffusive convection in nanofluids: a bio-nano-engineeringmodel," *Journal of Nanoengineering and Nanosystems*, 2012.

[36] V. P. Rathod and M. M. Channakote, "Effect of thickness of the porous material on the peristaltic pumping of a Jeffry fluid when the tube wall is provided with non- erodible porous lining", *International Journal of Mathematical Archive*, vol. 2, pp. 1-10, 2011.

[37] V. P. Rathod and N. G. Sridhar, "Peristaltic transport of couple stress fluid in uniform and non-uniform annulus through porous medium", *International Journal of Mathematical Archive*, vol. 3(4), pp. 1561-1574, 2012.

[38] V. P. Rathod and Laxmi Devindrappa, "Effects of heat transfer on the peristaltic MHD flow of a Bingham fluid through a porous medium in a channel", *International Journal of Biomathematics*. 7, art. id. 1450060-80, 2014.

[39] V. P. Rathod and Pallavi Kulkarni, "The influence of wall properties on peristaltic transport of dusty fluid through porous medium", *International Journal of Mathematical Archive,* vol. 2, pp. 1-13, 2011.

[40] V. P. Rathod and S. K. Asha, "Effect of couple stress fluid on peristaltic motion in a uniform and non-uniform annulus", *International Journal of Computer & Organization Trends,* vol. 3(11), pp. 482-490, 2013.

[41] S. Nadeem and N. S. Akbar, Peristaltic flow of a Jeffrey fluid with variable viscosity in an asymmetric channel, *Z. Naturforsch.*, vol.64a, pp. 713 – 722, 2009.

[42] S. R. Mahmoud, N. A. S. Afifi and H. M. Al-Isede, Effect of porous medium and magnetic field on peristaltic transport of a Jeffrey fluid, *International Journal of Mathematical Analysis*, vol. 5(21), pp. 1025 – 1034, 2011.

[43] K. Rajanikanth, S. Sreenadh, Y. Rajesh Yadav and A. Ebaid, MHD Peristaltic flow of a Jeffrey fluid in an asymmetric channel with partial slip, *Advances in Applied Science Research*, vol. 3 (6), pp. 3755 – 3765, 2012.

[44] N. S. Akbar, S. Nadeem and C. Lee, Characteristics of Jeffrey fluid model for peristaltic flow of chime in small intestine with magnetic field, *Results in Physics*, vol. 3, pp. 152–160, 2013.

[45] S. Nadeem, A. Riaz and R. Ellahi, Peristaltic flow of a Jeffrey fluid in a rectangular duct having compliant walls, *Chemical Industry & Chemical Engineering Quarterly*, vol.19 (3), pp. 399−409, 2013.

[46] S. Nadeem, A. Riaz, R. Ellahi and N. S. Akbar, Mathematical model for the peristaltic flow of Jeffrey fluid with nanoparticles phenomenon through a rectangular duct, *Applied Nanoscience*, vol. 4, pp. 613–624, 2014.

[47] N. Naga Jyothi, P. Devaki and S.Sreenadh, High frequency unsteady peristaltic flow of a Jeffrey fluid in uniform and tapered tube, *Elixir Fluid Dynamics*, vol. 60, pp. 16152 – 16166, 2013.

[48] A. Riaz, S. Nadeem, R. Ellahi and A. Zeeshan, Exact solution for peristaltic flow of Jeffrey fluid model in a three dimensional rectangular duct having slip at the walls, *Applied Bionics and Biomechanics*, vol. 11, pp. 81–90, 2014.

[49] D. G. S. Al-Khafajy, Effects of wall properties and heat transfer on the peristaltic transport of a Jeffrey fluid through porous medium channel, *Mathematical Theory and Modeling*, vol. 4(9), 86 – 99, 2014.

[50] N. T. M. El-dabe, G. M. Moatimid, M. A. Hassan, and D. R. Mostapha, Analytical solution of the peristaltic flow of a Jeffrey nanofluid in a tapered artery with mild stenosis and slip condition, *International Journal of Innovation and Applied Studies*, vol. 12 (1) pp. 1 – 32, 2015.

[51] N. Santhosh, G. Radhakrishnamacharya and A. J. Chamkha, Flow of a Jeffrey fluid through a porous medium in narrow tubes, *Journal of Porous Media*, vol. 18 (1), pp. 71–78, 2015.

[52] M. Majumder, N. Chopra, R. Andrews, and B. J. Hinds, "Nanoscale hydrodynamics: enhanced flow in carbon nanotubes," *Nature*, vol. 438, no. 7064, p. 44, 2005.

[53] N.S. Akbar and S. Nadeem, "Thermal and velocity slip effects on the peristaltic flow of a six constant Jeffrey's fluid model," *International Journal of Heat and Mass Transfer*, vol. 55, no. 15-16, pp. 3964–3970, 2012.

[54] A. Ebaid and E.H. Aly, Exact analytical solution of the peristaltic nanofluids flow in an asymmetric channel with flexible walls and slip condition: Application to the cancer treatment, Computational and Mathematical Methods in Medicine, vol. 2013, art. id. 825376, 2013.

[55] V. P. Rathod and D. Sanjeevkumar, Closed form solution of peristaltic flow of a magnetohydrodynamic nanofluid in an asymmetric channel having flexible walls, International Journal of Mathematical Archive, vol. 6, no.4, pp. 1-14, 2015.

Source of support: Nil, Conflict of interest: None Declared